An adaptive constrained multi-channel active noise control filter design approach using convex cone optimization

Yongjie Zhuang[1] and Yangfan Liu[2]
Ray W. Herrick Laboratories, Mechanical Engineering, Purdue University
177 S. Russell St., West Lafayette, IN 47907-2099, USA

ABSTRACT

In current practical active noise control (ANC) applications, solutions to three main technical challenges need to be sought: the requirement of a stable controller when acoustic feedback paths exist, a larger quiet zone, and adaptation to a time-varying environment. The imposed controller stability constraints can significantly increase the computational requirements and negatively impact the adaptation of ANC filters in real time. Multi-channel systems are usually needed if a larger quiet zone is required while the coupling between different channels can greatly lower the convergence rate of adaptive algorithms. In the current work, a multi-channel adaptive constrained ANC filter design method is proposed. The recently proposed convex cone formulation for ANC design is adopted to reduce the computational time of solving the constrained ANC filter design problem. The optimal filter coefficients are then redesigned continuously using convex optimization when the environment is time-varying. The experimental result shows that, compared with the traditional leaky FxLMS method, the proposed method has a faster convergence rate and a better steady-state noise control performance.

1. INTRODUCTION

Active noise control (ANC) is a technique that uses additional sources, such as loudspeakers, to produce an anti-sound to destructively interfere with unwanted noise. As a lightweight and highly configurable noise control strategy, ANC has been applied in various applications, including vehicles [1, 2], hearables [3–6], ventilation windows [7–9], etc.

A recent trend in ANC research focuses on the practical challenges of using the ANC in wider commercial applications. When designing ANC filters, solutions to three main technical challenges need to be sought: a) in complicated system operation environments where the generated anti-noise can contaminate the sensing of primary noise, the controller stability constraints are needed to ensure a stable performance [10, 11]; b) multi-channel systems are usually required to create a larger quiet

[1]zhuang32@purdue.edu

[2]yangfan@purdue.edu

zone which significantly increases the filter design problem dimensions: e.g., ANC solutions for vehicle cabins [12]; c) adaptive controllers are required for automatic adjustment to time-varying environments. Those three challenges may be coupled together leading to even greater challenges to design an ANC system. For example, multi-channel systems make the constraints formulations change from simple scalar equations to complicated matrices equations, which significantly increases the difficulties in filter coefficients computation; similarly, the coupling in different channels will significantly lower the convergence rate of controller adaption algorithms which leads to a degraded noise control performance; etc. Thus, an effective and efficient filter design method shall be developed to design adaptive multi-channel ANC filters under practical constraints.

Recently, a cone-programming-based ANC filter design method was proposed by Zhuang and Liu [13] that formulates the ANC filter design problem into a convex-constrained optimization problem and significantly improves the required computational time by several orders of magnitude with the help of a proposed reformulation of the ANC filter design problem to a convex cone programming problem. Then the numerical efficiency and reliability of this cone-programming-based ANC filter design method are further improved by using duality techniques [14]. However, this proposed method was applied to only non-adaptive applications so far. In this paper, an adaptive constrained ANC filter design method is developed based on this cone-programming-based ANC filter design method. The optimal ANC filter coefficients under practical constraints are computed by solving the cone-programming-based design method continuously using updated system responses.

The rest of this paper is organized as follows. The previously proposed cone-programming-based ANC filter design method and the traditional leaky FxLMS method are reviewed in Sections 2.1 and 2.2. Then the proposed adaptive constrained multi-channel ANC filter design under controller stability constraints is explained in Section 2.3. The experimental setup and results are discussed in Section 3. Conclusions of the current work and future works are drawn in Section 4.

2. THEORY

2.1. Review of the cone-programming-based multi-channel constrained ANC filter design method

The cone-programming-based ANC filter design method proposed in Zhuang and Liu's previous work [13,14] is reviewed in this section. The system block diagram is shown in Figure 1. This multi-channel system has N_r microphones, N_s loudspeakers, and N_e microphones as reference sensors, secondary sources, and error sensors respectively. In Figure 1, $\vec{\mathbf{x}}$ denotes the primary noise signals. $\vec{\mathbf{r}}$ denotes the reference signals collected by the reference microphones which include sound from both the primary sources and contribution from the secondary sources via acoustic feedback path $\mathbf{G}_s$. $\vec{\mathbf{y}}$ denotes the output of the controller $\mathbf{H}$. $\vec{\mathbf{d}}$ denotes the disturbance signals, i.e., noise signals from only primary sources that are collected by the error microphones when the secondary sources are turned off. $\vec{\mathbf{e}}$ denotes the residue noise signals after the ANC system is activated, and the power of $\vec{\mathbf{e}}$ is to be minimized in the ANC filter design process. An internal model control structure can be used in the controller $\mathbf{H}$ [12, 15] to cancel the effect of acoustic feedback path, where $\hat{\mathbf{G}}_s$ is an estimate of the acoustic feedback path, $\mathbf{G}_s$. $\hat{\mathbf{G}}_s$ is assumed to be a perfect model (i.e., $\hat{\mathbf{G}}_s = \mathbf{G_s}$), when operating in a nominal working condition, this system will become a standard feedforward system (as shown in Figure 2). $\mathbf{G}_e$ denotes the acoustical responses matrix from the secondary sources to the error sensors. $\mathbf{W}_x$ denotes the frequency response matrix of the multi-channel ANC filters.

In the current work, FIR filter structure is used for ANC filters whose frequency responses are

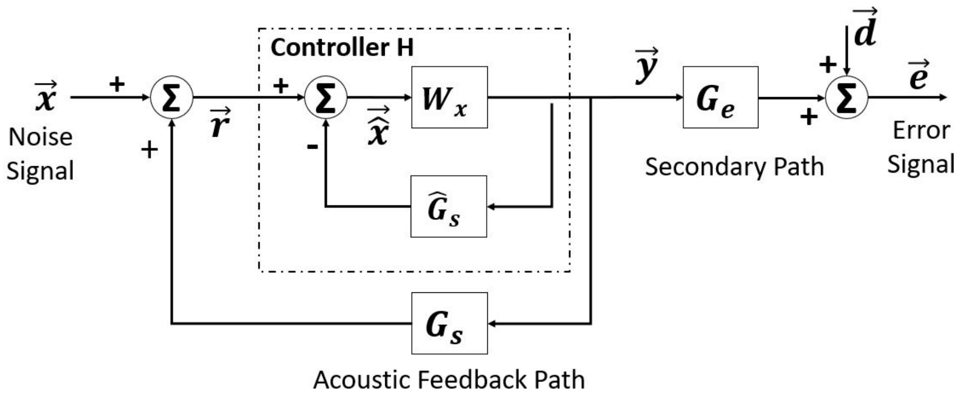

Figure 1: The block diagram of a multi-channel ANC system with the acoustic feedback path and internal model structure.

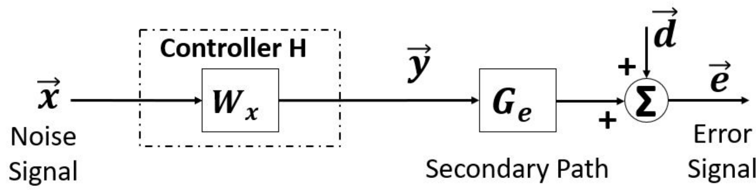

Figure 2: The block diagram of a multi-channel ANC system assuming the estimate of the acoustic feedback path is perfect in nominal condition.

$\mathbf{W}_x$. Thus, at any frequency, each element of $\mathbf{W}_x$ is a linear function of the FIR filter coefficients $\vec{\mathbf{w}}_{F_{i,j}}$ which are calculated in the filter design process [13, 14]:

$$\mathbf{W}_{x_{i,j}}(f) = \vec{\mathbf{F}}_z^{\mathrm{T}}(f)\vec{\mathbf{w}}_{F_{i,j}}, \tag{1}$$

where

$$\vec{\mathbf{F}}_z(f) = \begin{bmatrix} 1 & e^{-j2\pi f \frac{1}{f_s}} & e^{-j2\pi f \frac{2}{f_s}} & \dots & e^{-j2\pi f \frac{N_t-1}{f_s}} \end{bmatrix}^{\mathrm{T}};$$

f denotes the frequency; f_s denotes the sampling frequency. $\mathbf{W}_{x_{i,j}}(f)$ denotes the element at the i-th row and j-th column of frequency response matrix $\mathbf{W}_x(f)$. T denotes the matrix transpose operation. Each $\vec{\mathbf{w}}_{F_{i,j}}$ is a column vector that includes the N_t ANC FIR filter coefficients associated with the i-th output and j-th input channel [13, 14].

The objective function can be formulated as the total power of error signals across the desired frequency bands using a convex quadratic function [13]:

$$\vec{\mathbf{w}}^{\mathrm{T}} \left(\sum_{k=1}^{N_f} \mathbf{A}_J(f_k) \right) \vec{\mathbf{w}} + \sum_{k=1}^{N_f} \vec{\mathbf{b}}_J^{\mathrm{T}}(f_k)\, \vec{\mathbf{w}} \tag{2}$$

where $\vec{\mathbf{w}}$ is the variable vector to be solved and is constructed by stacking FIR filter coefficients of all channel pairs. In Equation 2: [13]

$$\mathbf{A}_J(f_k) = \Re\left(\left(\mathbf{G}_e^{\mathrm{H}}(f_k)\mathbf{G}_e(f_k)\right) \otimes \mathbf{S}_{xx}^{\mathrm{T}}(f_k) \otimes \left(\vec{\mathbf{F}}_z^{*}(f_k)\vec{\mathbf{F}}_z^{\mathrm{T}}(f_k)\right)\right),$$
$$\vec{\mathbf{b}}_J(f_k) = 2\Re\left(\mathrm{vec}\left((\mathbf{S}_{xd_e}(f_k)\mathbf{G}_e(f_k)) \otimes \vec{\mathbf{F}}_z(f_k)\right)\right),$$
$$\vec{\mathbf{w}} = \begin{bmatrix}\vec{\mathbf{w}}_{F_{1,1}}^{\mathrm{T}} & \dots & \vec{\mathbf{w}}_{F_{1,N_r}}^{\mathrm{T}} & \vec{\mathbf{w}}_{F_{2,1}}^{\mathrm{T}} & \dots & \vec{\mathbf{w}}_{F_{N_s,N_r}}^{\mathrm{T}}\end{bmatrix}^{\mathrm{T}},$$

where H denotes complex conjugate transpose operation, $\otimes$ denotes the Kronecker product, $*$ denotes the complex conjugate operation, and vec() denotes the vectorization operation that converts a matrix to a vector by stacking the columns of this matrix [16]; $\mathbf{S}_{xx}(f_k)$ is the cross-spectral density matrix of $\vec{\mathbf{x}}$ at frequency f_k; $\mathbf{S}_{xd}(f_k)$ is the cross-spectral density matrix between the primary noise signals $\vec{\mathbf{x}}$ and the disturbance signals $\vec{\mathbf{d}}$ at frequency f_k; $\Re()$ denotes the real part of a complex number (or matrix).

Even if the estimate of the acoustic feedback path $\hat{\mathbf{G}}_s$ is assumed to be perfect in nominal operating conditions, the stability issue caused by the closed loop, $\mathbf{W}_x(f_k)\hat{\mathbf{G}}_s(f_k)$, in the controller $\mathbf{H}$ should still be considered. The following constraint can be applied to ensure the stability of controller $\mathbf{H}$: [13]

$$\max\left(\lambda\left(\frac{-\mathbf{W}_x(f_k)\hat{\mathbf{G}}_s(f_k) - \hat{\mathbf{G}}_s(f_k)^{\mathrm{H}}\mathbf{W}_x(f_k)^{\mathrm{H}}}{2}\right)\right) - (1-\epsilon_s) \leq 0, \tag{3}$$

where $\lambda()$ denotes the eigenvalues values of a matrix; ϵ_s is a small positive constant to ensure strict stability. More details on this convex formulation of the ANC filter design problem can be referred to reference [13]. Equation 2 and Equation 3 can then be reformulated into their simplified dual form to further improve the numerical efficiency and reliability [14]. More details on the dual reformulation can be referred to reference [14]. It was demonstrated in Zhuang and Liu's work [13, 14] that this formulation can reduce a typical constrained ANC filter design problem solution time from the order of hours to seconds, which makes it possible to be used in adaptive control by continuously solving the constrained ANC filter design problem with updated measured system responses.

2.2. Review of traditional leaky FxLMS method

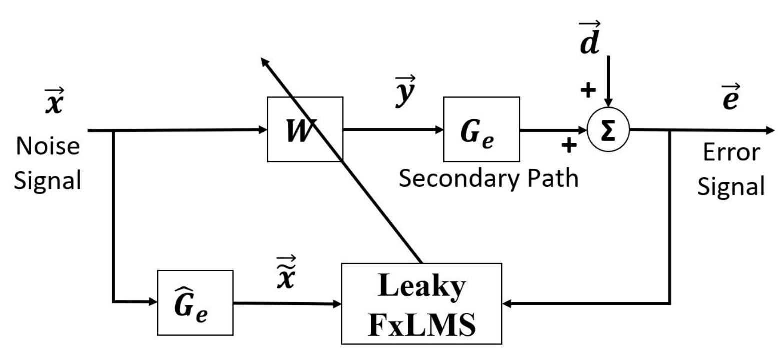

Figure 3: The block diagram of a traditional leaky FxLMS method in ANC systems.

The traditional leaky FxLMS method is a common approach for designing adaptive constrained ANC filters. Figure 3 shows a leaky FxLMS block diagram with the assumption that $\hat{\mathbf{G}}_s$ is a perfect model in the nominal operating condition. $\vec{\tilde{\mathbf{x}}}$ is obtained by filtering the noise signals $\vec{\mathbf{x}}$ using the estimate of the secondary path responses $\hat{\mathbf{G}}_e$. For each channel of the control filter, the filter coefficients can be updated at $(n+1)$-th iteration using:

$$w_{i,j,k}^{(n+1)} = w_{i,j,k}^{(n)} - \alpha\left(\sum_{l=1}^{N_e} \tilde{x}_{i,j,l}(n-k)e_l(n) + \beta w_{i,j,k}^{(n)}\right), \tag{4}$$

where the indices denote i-th control speaker output, j-th reference microphone input, k-th coefficient in the noise control filter channel, and l-th error microphone input; α is the step size that controls the convergence rate of the adaptive algorithm; β is the leakage factor. When leakage factor β is large enough, most of the common constraints on controllers can be satisfied [10, 11, 17–23].

2.3. Proposed adaptive constrained multi-channel ANC filter design method

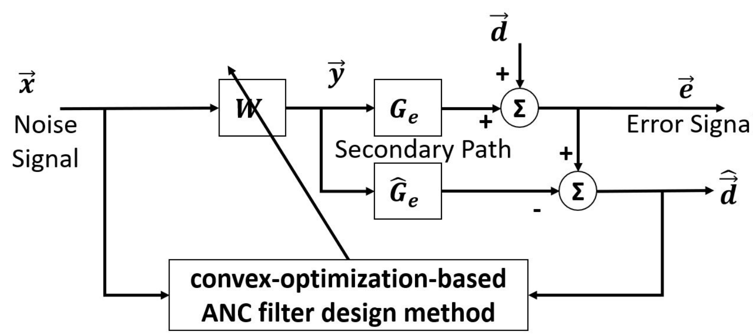

Figure 4: Block diagram of the proposed multi-channel adaptive constrained ANC filter design method.

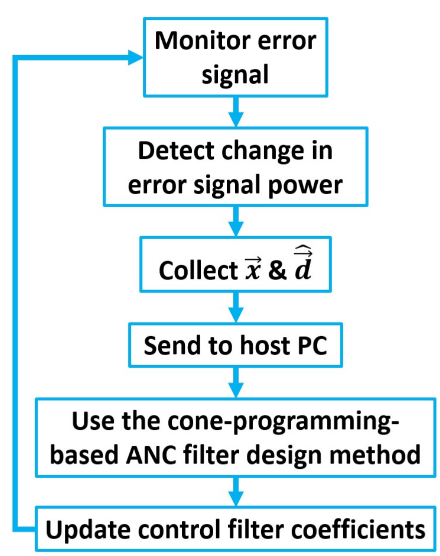

Figure 5: A flowchart of the proposed multi-channel adaptive constrained ANC filter design method.

The block diagram of the proposed adaptive constrained multi-channel ANC filter design method is shown in Figure 4 when $\hat{\mathbf{G}}_s$ is assumed to be a perfect model in the nominal operating condition. Similar to the leaky FxLMS method, an estimate of the secondary path, $\hat{\mathbf{G}}_e$, is also required in real-time implementation. The $\hat{\mathbf{G}}_e$ is used in the proposed method to obtain the estimate of the disturbance signal $\hat{\vec{\mathbf{d}}}$ so that the cross-spectral density matrix of $\vec{\mathbf{x}}$ and $\vec{\mathbf{d}}$ can be estimated during real-time operation. The flowchart of the proposed method is shown in Figure 5. When the change of the error signal power exceeds a prescribed threshold, it indicates a change occurs in system response or environment characteristics, the signals $\vec{\mathbf{x}}$ and $\hat{\vec{\mathbf{d}}}$ can then be collected for a short period (e.g., 10 seconds) of time and are used to compute updated system responses. Then the cone-programming-based ANC filter design method can be used to compute the optimal ANC filter coefficients using the updated system responses. By continuously implementing this procedure, the optimal ANC filter coefficients under practical constraints can be updated in a time-varying environment.

3. EXPERIMENTAL RESULTS

3.1. Experimental setup

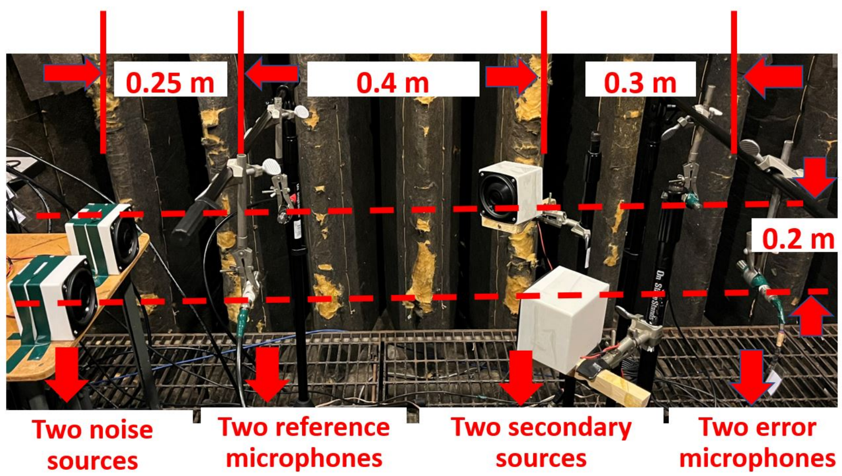

Figure 6: A picture of the experimental setup.

A multi-channel ANC system was constructed in an anechoic chamber to investigate the ANC performance and related system characteristics of the proposed method. The experiment setup is shown in Figure 6. Two speakers were used as primary noise sources and two speakers as secondary sources (control sources). Two reference microphones and two error microphones were used. The key dimensions between components are also shown in Figure 6. The data acquisition and control algorithm were implemented using dSPACE MicroLabBox (MLBX_1302T). A high sampling rate (9 kHz) was used in the data acquisition process to reduce the electronic delay in the signal paths. After appropriately designed anti-aliasing and reconstruction filters, the measured signal is downsampled to 3 kHz which is the controller operation sampling rate. The desired noise control band was from 100 Hz to 1.4 kHz. In each channel, the filter lengths of ANC control filters, estimated secondary paths, and the estimated acoustic feedback paths were all chosen to be 64.

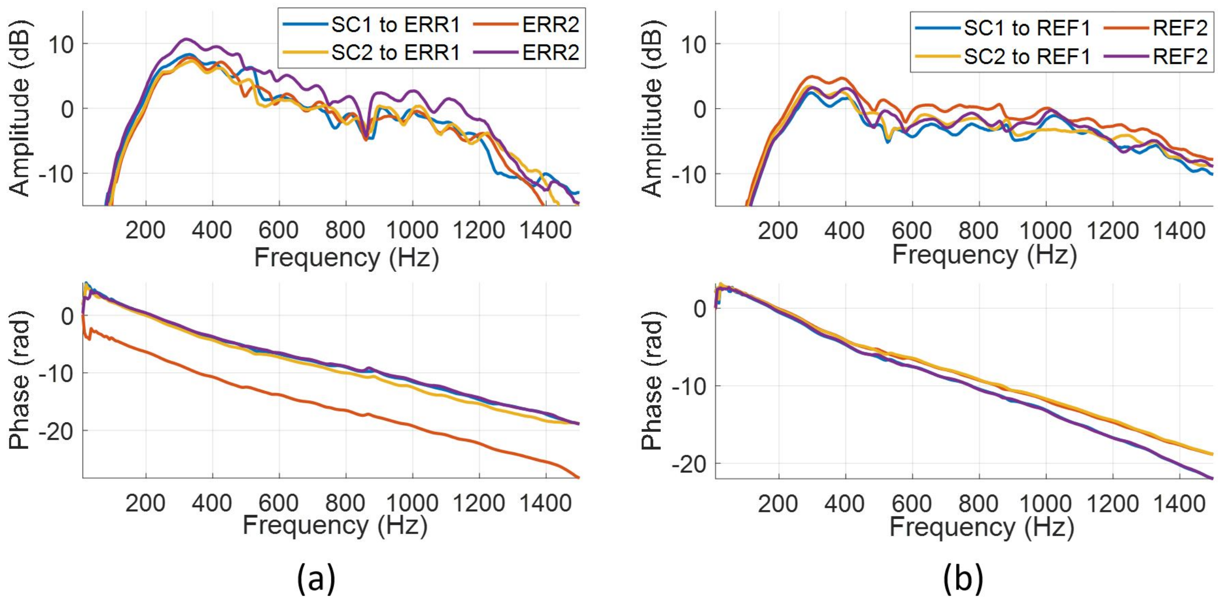

Figure 7: The measured frequency responses of (a) secondary paths $\mathbf{G}_e$, and (b) acoustic feedback paths $\mathbf{G}_s$. "SC1" and "SC2" represent two control speakers; "ERR1" and "ERR2" represent two error microphones; "REF1" and "REF2" represent two reference microphones.

The measured frequency responses of the secondary paths $\mathbf{G}_e$ and the acoustic feedback paths $\mathbf{G}_s$ are shown in Figure 7. From Figure 7, the amplitudes of the acoustic feedback paths' frequency responses are approximately in the same order as those of the secondary paths. This demonstrates that the acoustic feedback paths are strong and the unconstrained optimal ANC filter may cause an unstable closed loop $\mathbf{W}_x(f_k)\hat{\mathbf{G}}_s(f_k)$. In practice, stability constraints should be considered by either using the constraint Equation 3 in the cone-programming-based ANC design method or tuning the leakage factor β in the leaky FxLMS method.

To create a time-varying environment in the experiment, primary noise source signals with different frequency spectral characteristics were generated. When using the two noise source speakers to generate noise signals, two independent white noise signals were generated digitally first and then they were filtered by two different digital filters. The frequency response magnitudes of the two digital filters are shown in Figure 8. Specifically, there were two types of primary noise signal characteristics: (a) full-band case: both noise source speakers play independent noise signals from 100 Hz to 1450 Hz; (b) half-band case: one noise source speaker plays noise signal from 100 Hz to 950 Hz and another noise source speaker plays noise signal from 600 Hz to 1450 Hz. During the experiment, the noise signals can be switched from the full-band case to the half-band case to create a time-varying environment.

3.2. Comparison of ANC performance

When using the leaky FxLMS method, the leakage factor β was tuned to be the smallest value that still produces a stable controller, which was 1×10^{-5} in this experiment. The step length α was tuned to be the largest value that still satisfies the convergence of the algorithm, which was 0.1 in this experiment. Thus, in the experiment, the traditional leaky FxLMS was tuned to result in the best

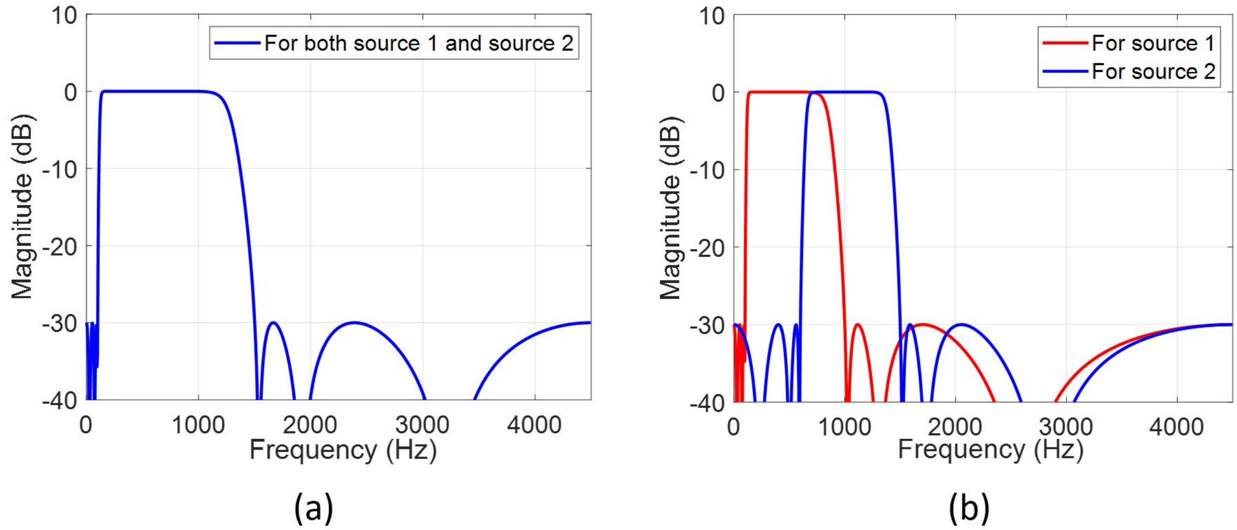

Figure 8: The designed frequency responses of (a) full-band case: digital filter passband is from 100 Hz to 1450 Hz, and (b) half-band case: one digital filter passband is from 100 Hz to 950 Hz and another digital filter passband is from 600 Hz to 1450 Hz.

achievable ANC performance.

When implementing the proposed method, a 5 Hz frequency resolution was used in the filter design formulations [13, 14] (i.e., the equation 2 and 3). To choose an appropriate updating interval for the proposed method, the approximate problem solution time for the cone-programming-based formulation in this experimental setup is required. Thus, 100 cases using the same problem dimension in this experimental setup were first generated with random variations based on measured system responses and then tested in MATLAB R2021a in the host PC (CPU: 11th Gen Intel(R) Core(TM) i7-1185G7 @ 3.00GHz 1.80 GHz; RAM 32 GB; 64-bit operating system). The mean value and 3-sigma limit (99.7%) of the required computational time (in total CPU time summing across all threads) is 5.0 ± 1.8 seconds for solving the cone-programming-based ANC filter design problem, and 0.19 ± 0.16 seconds for computing the system responses spectra from collected data. Thus, in this experimental setup, 10 seconds were used for data collection to include sufficient data to compute the system response spectra, and 10 seconds were used for filter coefficient computation to allow sufficient time in solving the proposed cone-programming-based ANC design formulation and updating the ANC filter in the controller.

The comparison of ANC performance in the time domain using the traditional leaky FxLMS method and the proposed method is shown in Figure 9. The full-band case was first used to drive the primary noise source speakers, the traditional FxLMS method started to update its filter coefficients and the noise power began to decrease. For the proposed method, immediately after the system changed from a deactivated state to an operating state, 10 seconds were used for collecting signals and another 10 seconds were used for computing the optimal filter coefficients. After the filter coefficients in the controller were updated using the computed optimal filter coefficients, the noise power using the proposed method immediately reached the optimal power level. Thus, the convergence time using the proposed method (in the current work, it is defined as the time from the moment when a change in system or environment characteristics occurs to the moment when the optimal control performance

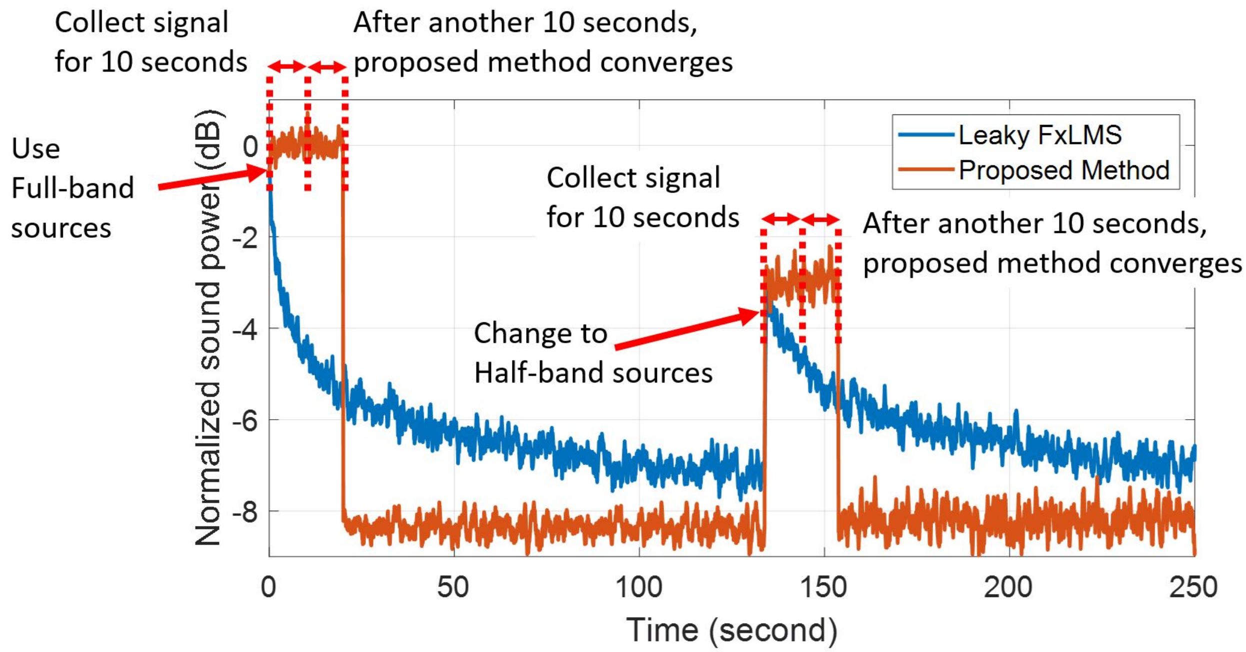

Figure 9: The comparison of ANC performance in the time domain using the traditional leaky FxLMS method and the proposed method. The power is normalized by the total error signal power at full-band noise sources case without using an ANC system and the reference value for the dB scale is 1.

is achieved) is 20 seconds in this experimental setup. However, the convergence time is more than 120 seconds for the traditional leaky FxLMS method. When both methods converge, the noise source speakers will switch to the half-band case which causes a significant increase in the residual noise power level, because the current filter coefficients are not optimal after the change of primary noise signal characteristics. A similar process started again where the filter coefficients were updated by using both methods. Note that due to the limit in the data communication capability between the host PC and the controller, the ANC performance using the proposed method is measured separately for different stages and plotted in the same figure (i.e., the code loading period when updating the filter coefficients is truncated from the figure to match the time indices because the device will be temporarily shut off while loading the code). This implementation won't affect the conclusion because the proposed method is essentially stationary in each stage. To better compare the ANC performance in the steady state, Figure 10 shows the ANC performance in the frequency domain when both the traditional leaky FxLMS and the proposed method converge for (a) full-band case, and (b) half-band case. In this figure, "ANC OFF" denotes the original noise power level when the ANC system is not activated. Figure 9 and Figure 10 demonstrate that the proposed method has a faster convergence rate and better steady-state ANC performance compared with the traditional FxLMS method.

4. CONCLUSIONS

In this paper, an adaptive multi-channel filter design approach is proposed for active noise control applications under controller stability constraints. The optimal ANC filter coefficients are updated by solving a previously proposed cone-programming-based ANC filter design method continuously

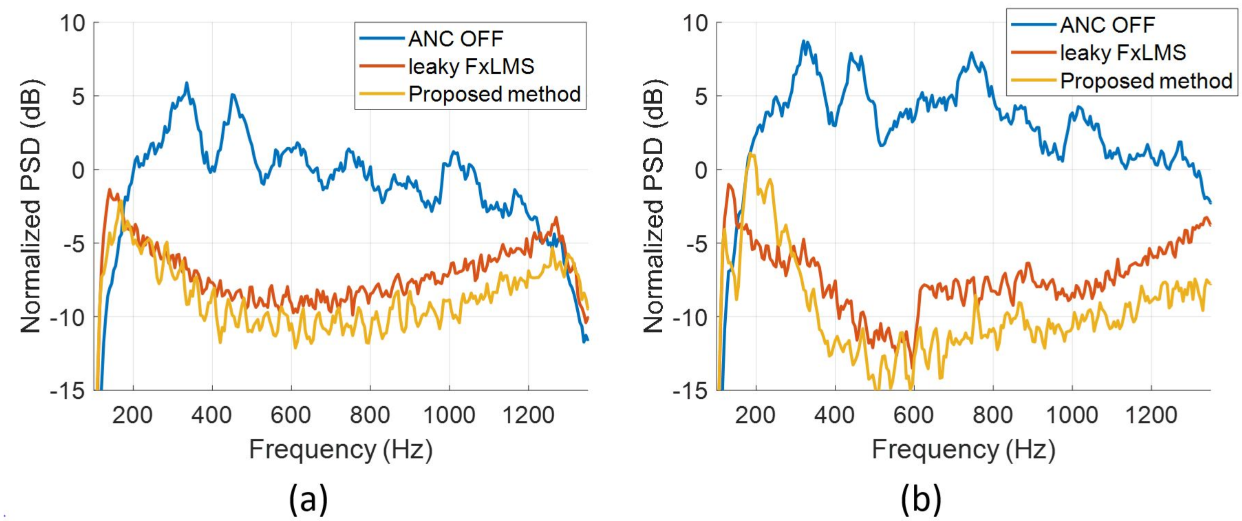

Figure 10: The comparison of ANC performance in the frequency domain when both the traditional leaky FxLMS and the proposed method converge for (a) full-band case, and (b) half-band case.

using the updated system response measurements. Compared with the traditional leaky FxLMS method, the proposed method has a faster convergence rate and better steady-state ANC performance. The proposed method can be suitable for ANC applications where signal characteristics rapidly change from one steady state to another different steady state: e.g., equipment speeds are switched among some predetermined values during the operation of rotating machinery; or when various products share the same host server in multi-task applications that the control filter coefficients can be updated in a short time using the powerful server without adding too much marginal cost: e.g., the smart home/office application.

In the future, other techniques can be incorporated into the proposed method to further improve its computational efficiency. For example, the optimal filter coefficients under a previous environmental condition can provide a better choice of an initial guess of the filter coefficients for a perturbed environment after environment changes occur, i.e., the warmstarting techniques [24] may be applied. The proposed method can also extend to wider applications, e.g., online secondary (or acoustic feedback) paths identification techniques can be incorporated into the proposed method when the secondary (or acoustic feedback) paths are time-varying.

ACKNOWLEDGEMENTS

The authors thank Beijing Ancsonic Technology Co. Ltd for providing financial support.

REFERENCES

[1] S Zhang, YS Wang, H Guo, C Yang, XL Wang, and NN Liu. A normalized frequency-domain block filtered-x LMS algorithm for active vehicle interior noise control. *Mechanical Systems and Signal Processing*, 120:150–165, 2019.

[2] Woomin Jung, Stephen J Elliott, and Jordan Cheer. Local active control of road noise inside a vehicle. *Mechanical Systems and Signal Processing*, 121:144–157, 2019.

[3] Bhan Lam, Woon-Seng Gan, DongYuan Shi, Masaharu Nishimura, and Stephen Elliott. Ten questions concerning active noise control in the built environment. *Building and Environment*, 200:107928, 2021.

[4] Fengyan An, Qianqian Wu, and Bilong Liu. Feedback controller optimization for active noise control headphones considering frequency response mismatch between microphone and human ear. *Applied Sciences*, 12(3):977, 2022.

[5] Sen M Kuo, Yi-Rou Chen, Cheng-Yuan Chang, and Chien-Wen Lai. Development and evaluation of light-weight active noise cancellation earphones. *Applied Sciences*, 8(7):1178, 2018.

[6] Yongjie Zhuang and Yangfan Liu. A constrained optimal hear-through filter design approach for earphones. In *INTER-NOISE and NOISE-CON Congress and Conference Proceedings*, volume 263, pages 1329–1337. Institute of Noise Control Engineering, 2021.

[7] Jianjun He, Bhan Lam, Dongyuan Shi, and Woon Seng Gan. Exploiting the underdetermined system in multichannel active noise control for open windows. *Applied Sciences*, 9(3):390, 2019.

[8] Hsiao Mun Lee, Yuting Hua, Zhaomeng Wang, Kian Meng Lim, and Heow Pueh Lee. A review of the application of active noise control technologies on windows: Challenges and limitations. *Applied Acoustics*, 174:107753, 2021.

[9] Liangfen Du, Siu-Kit Lau, Siew Eang Lee, and Martin Konrad Danzer. Experimental study on noise reduction and ventilation performances of sound-proofed ventilation window. *Building and Environment*, 181:107105, 2020.

[10] Fengyan An, Yin Cao, Ming Wu, Hongling Sun, Bilong Liu, and Jun Yang. Robust wiener controller design with acoustic feedback for active noise control systems. *The Journal of the Acoustical Society of America*, 145(4):EL291–EL296, 2019.

[11] Lifu Wu, Xiaojun Qiu, and Yecai Guo. A simplified adaptive feedback active noise control system. *Applied Acoustics*, 81:40–46, 2014.

[12] Jordan Cheer and Stephen J Elliott. Multichannel control systems for the attenuation of interior road noise in vehicles. *Mechanical Systems and Signal Processing*, 60:753–769, 2015.

[13] Yongjie Zhuang and Yangfan Liu. Constrained optimal filter design for multi-channel active noise control via convex optimization. *The Journal of the Acoustical Society of America*, 150(4):2888–2899, 2021.

[14] Yongjie Zhuang and Yangfan Liu. A numerically stable constrained optimal filter design method for multichannel active noise control using dual conic formulation. *The Journal of the Acoustical Society of America*, 152(4):2169–2182, 2022.

[15] S.J. Elliott. *Signal Processing for Active Control*, chapter 6, pages 271–327. Signal Processing and its Applications. Academic Press, London, 2001.

[16] Kaare Brandt Petersen and Michael Syskind Pedersen. *The Matrix Cookbook*, chapter 10.2.2, page 60. November 2012. (Last viewed 03/08/2023) Version 20121115.

[17] Dongyuan Shi, Woon-Seng Gan, Bhan Lam, and Xiaoyi Shen. Comb-partitioned frequency-domain constraint adaptive algorithm for active noise control. *Signal Processing*, 188:108222, 2021.

[18] Dongyuan Shi, Woon-Seng Gan, Bhan Lam, Shulin Wen, and Xiaoyi Shen. Optimal output-constrained active noise control based on inverse adaptive modeling leak factor estimate. *IEEE/ACM Transactions on Audio, Speech, and Language Processing*, 29:1256–1269, 2021.

[19] José CM Bermudez and Márcia H Costa. Optimum leakage factor for the mov-lms algorithm in nonlinear modeling and control systems. In *2002 IEEE International Conference on Acoustics, Speech, and Signal Processing*, volume 2, pages II–1393. IEEE, 2002.

[20] Walter J Kozacky and Tokunbo Ogunfunmi. An active noise control algorithm with gain and power constraints on the adaptive filter. *EURASIP Journal on Advances in Signal Processing*, 2013(1):1–12, 2013.

[21] Walter J Kozacky and Tokunbo Ogunfunmi. A cascaded iir–fir adaptive anc system with output power constraints. *Signal processing*, 94:456–464, 2014.

[22] Chaohui Zhou, Haishan Zou, and Xiaojun Qiu. A frequency band constrained filtered–x least mean square algorithm for feedback active control systems. *The Journal of the Acoustical Society of America*, 148(4):1947–1951, 2020.

[23] Lifu Wu, Xiaojun Qiu, and Yecai Guo. A generalized leaky fxlms algorithm for tuning the waterbed effect of feedback active noise control systems. *Mechanical Systems and Signal Processing*, 106:13–23, 2018.

[24] Yongjie Zhuang, Zhuang Mo, and Yangfan Liu. Warmstarting the constrained optimal filter design problem for active noise control systems in conic formulation. In *INTER-NOISE and NOISE-CON Congress and Conference Proceedings*, volume 264, pages 259–269. Institute of Noise Control Engineering, 2022.